JOURNAL OF MATERIALS SCIENCE 30 (1995) 3734–3745

Characterization of SiC whiskers

L. K. FREVEL, C. K. SAHA, D. R. PETERSEN
Dow Corning Corporation, Midland, MI 48686, USA

The composition and microstructure of SiC whiskers from three different suppliers were studied to understand their physical and chemical properties. The following analytical methods were utilized: complete chemical analysis, morphological examination by scanning electron microscopy and by high-resolution transmission electron microscopy, selected-area electron diffraction, X-ray diffraction, and thermogravimetric analysis of the oxidation rate of the three SiC whiskers at 1050 °C in oxygen and at 1150 °C in air.

1. Introduction

Silicon carbide whiskers are promising candidates for use as reinforcements for ceramic matrices such as SiC, Si_3N_4, and Al_2O_3. The benefits of incorporating such reinforcing agents in Al_2O_3, as well as in Si_3N_4 matrices, have already been demonstrated [1–5] to yield enhanced toughness, strength, and creep performance. The current whisker characterization at Dow Corning is aimed at supporting development of a scientific approach to maximize the reinforcing properties of these whiskers in organosilicon polymer-derived matrices.

It has been reported [6, 7] that SiC whiskers vary extensively with respect to morphology and bulk/surface chemistry from one supplier to another as well as from batch to batch. These differences have been reported to have dramatic effects on the processing and final properties of whisker-containing composites [8, 9].

The present work focused on the concerted applications of the following analytical methods: analytical chemistry, scanning electron microscopy (SEM), transmission electron microscopy (TEM), selected-area electron diffraction (SAED), X-ray diffraction (XRD), and thermogravimetric analysis (TGA).

2. Experimental procedure

Silicon carbide whiskers were procured from three commercial sources: Tateho America Inc., Tokai Carbon America Inc., and American Matrix Inc. All three samples were studied by the different techniques.

2.1. Chemical analysis

Carbon analysis was performed on a Control Equipment Corporation 240-XA Element Analyser. Oxygen analysis was determined on a LECO oxygen analyser equipped with an oxygen determinator 316 (Model 783700), and an electrode furnace EF 100. Silicon was determined by a fusion technique which consisted of converting the silicon material to soluble forms of silicon and analysing the solute for total silicon by atomic absorption spectroscopy. Trace impurities

TABLE I Elemental data (wt % except where marked) on bulk SiC whiskers

Elements	Tateho		Tokai		American Matrix
	Present work	Karasek *et al.* [6]	Present work	Karasek *et al.* [6]	
Si	67.2	–	68.83	–	67.3[a] / 65.51[b]
C	29.2	29.2(2)	29.0	28.6(2)	29.4[b]
O	0.48	0.56(4)	0.97	1.85(4)	1.22[b]
B	< 0.05	–	< 0.05		0.33[b]
Ca	< 100 p.p.m.	0.099	> 100 p.p.m.	–	> 100 p.p.m.
Mn	–	0.015	< 100 p.p.m.	< 0.005	–
Al	< 0.05	0.12	0.14	< 0.05	0.06
Fe	> 100 p.p.m.	0.045	> 100 p.p.m.	0.023	> 100 p.p.m.
Mg		0.007		< 0.005	
Na		< 0.4		< 0.4	
K	~ 0.05	–			
Co	> 100 p.p.m.	–	–	0.29	–
Ti	< 100 p.p.m.	0.090	< 100 p.p.m.	0.14	< 100 p.p.m.
Zr	–	0.11	< 100 p.p.m.	–	< 100 p.p.m.

[a] Na_2O_2 method.
[b] KOH method.

0022–2461

were determined by the X-ray fluorescence (XRF) technique. Energy dispersive X-ray spectroscopy (EDS) on the Tateho SiC whiskers confirmed the presence of aluminium, calcium, iron and potassium. Table I summarizes the elemental analyses on the three different SiC whiskers.

2.2. Morphological examinations

Scanning electron microscopy with a Jeol T300 instrument yielded useful information on the aspect ratio, intergrowth twinning, surface roughness, and clustering of various whiskers. Sample preparation involved dispersing the SiC whiskers in pure toluene, placing a drop of suspension on an aluminium foil substrate and letting the toluene evaporate. Magnification of 10^3–10^4 was employed. Figs 1–3 are micrographs pertaining to Tateho SiC whiskers. To ascertain the effect of light grinding, a 50 mg sample of whiskers was comminuted in a boron carbide mortar for 5 min. Figs 4 and 5 show the morphology of the Tokai SiC whiskers; Figs 6 and 7 refer to American Matrix SiC whiskers.

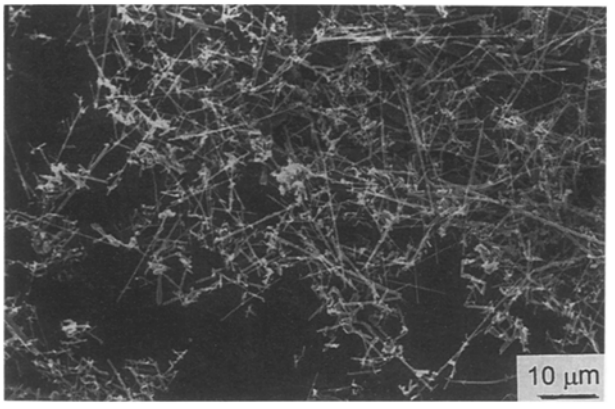

Figure 1 Scanning electron micrograph of Tateho SiC whiskers as received.

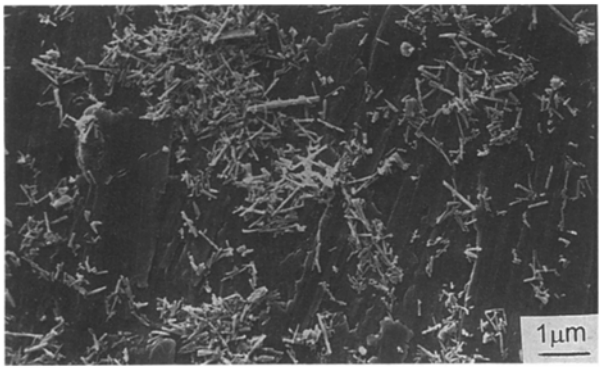

Figure 2 Scanning electron micrograph of Tateho SiC whiskers after grinding.

TEM was performed on a Jeol 1200 ATEM. A small portion of whiskers was sprinkled on to a carbon-coated copper grid and any non-adhering excess of whiskers was removed by gently tapping the tweezers holding the grid. For SAED, the electron beam diameter was adjusted to 2–5 μm and the selected-area aperture to 0.5 μm (exposure time 20 s, 120 kV electron beam). Figs 8–10 show ×70 000 enlargement of Tateho SiC whiskers. For the Tokai material, Fig. 11 shows a ×32 000 enlargement of several joined whiskers. Fig. 12 reveals the 1.6 nm striations in

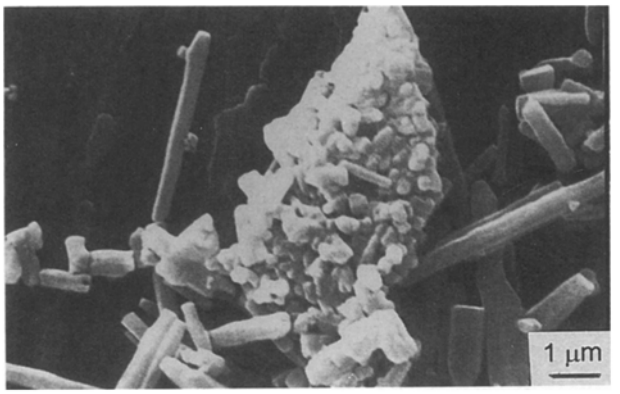

Figure 3 Scanning electron micrograph of cluster of Tateho SiC whiskers.

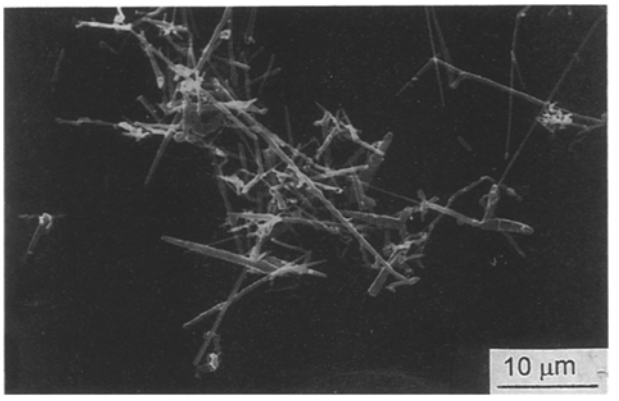

Figure 4 Scanning electron micrograph of Tokai SiC whiskers.

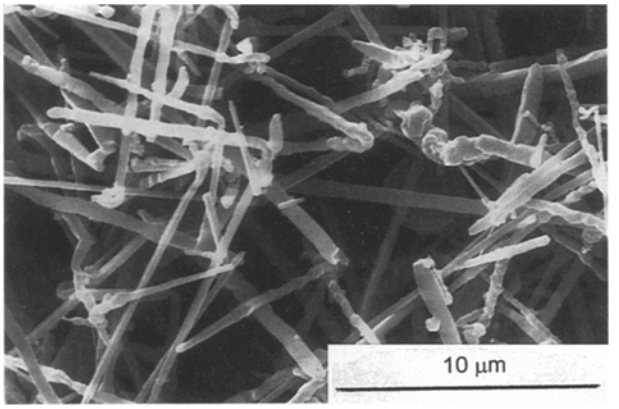

Figure 5 Scanning electron micrograph of Tokai SiC whiskers (larger magnification).

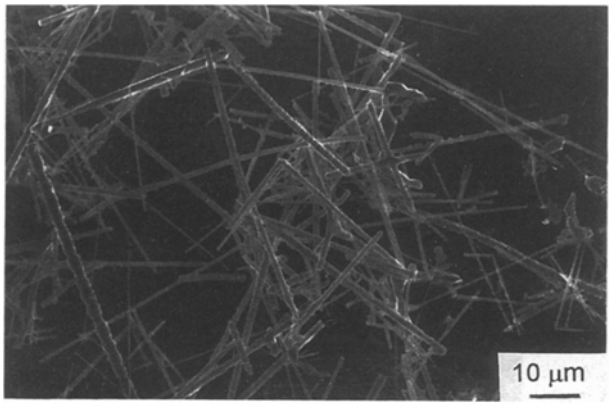

Figure 6 Scanning electron micrograph of American Matrix SiC whiskers.

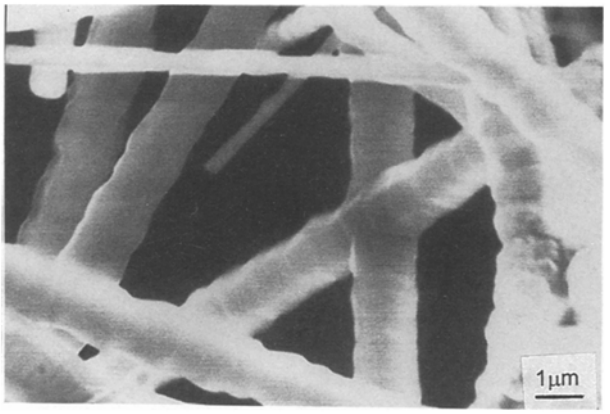

Figure 7 Scanning electron micrograph of American Matrix SiC whiskers (larger magnification).

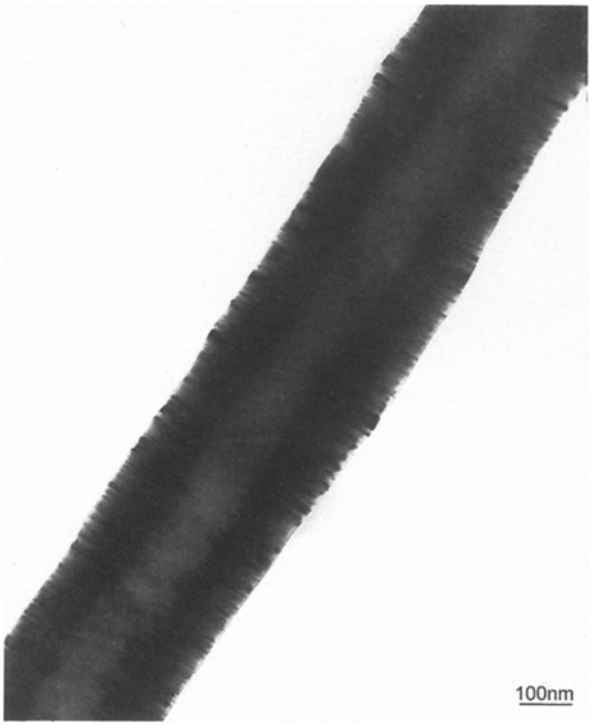

Figure 8 Transmission electron micrograph of Tateho SiC whiskers showing hollow core and stacking faults.

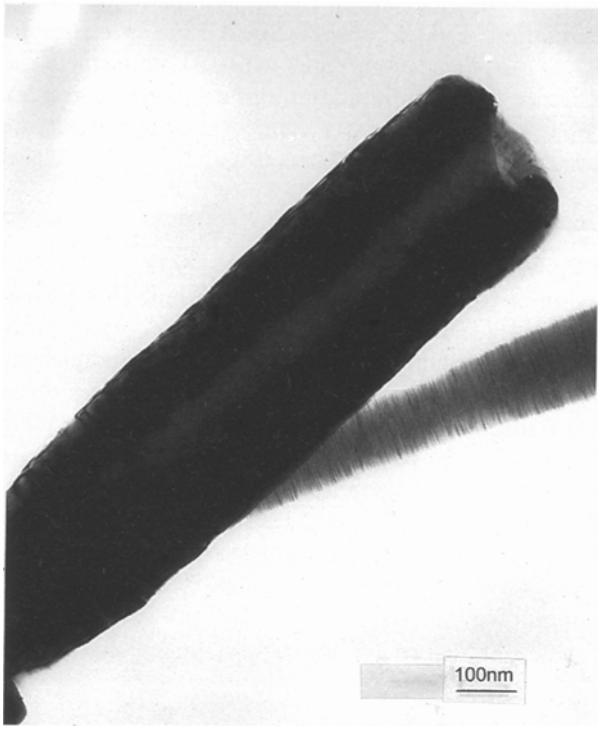

Figure 9 Transmission electron micrograph of Tateho SiC whiskers of different thickness.

Figure 10 Transmission electron micrograph of Tateho SiC whiskers. Almost end-on view shows core diameter.

a $\times 260\,000$ enlargement of the tip of a smooth fibre. The thin coating on an American Matrix SiC whisker is clearly seen in Fig. 13. The morphological data of the three samples of SiC whiskers are summarized in Table II.

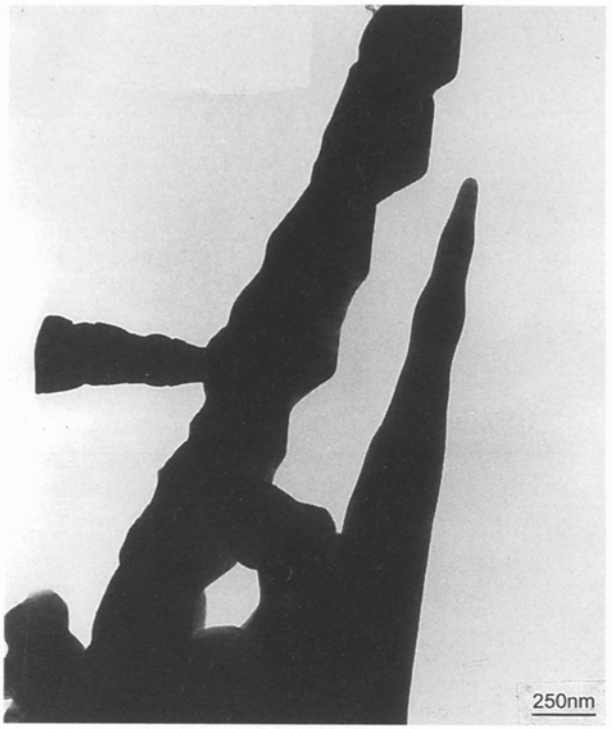

Figure 11 Transmission electron micrograph of several Tokai whiskers.

Figure 13 Transmission electron micrograph of American Matrix SiC whiskers possessing a thin coating (3 nm).

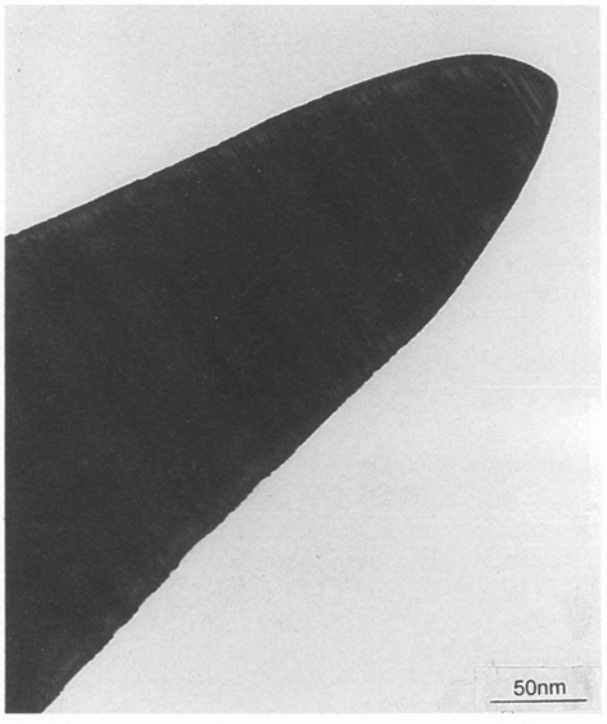

Figure 12 Transmission electron micrograph of tip of Tokai SiC whiskers.

To ascertain the crystallite-size distribution, film data were obtained in an evacuated Gandolfi camera (114.7 mm diameter) with 0.3 mm diameter slit. The self-supporting powder layer (0.2 mm thick) of as-received SiC whiskers was held in a special holder which was not exposed to the primary X-ray beam (CuK_α radiation, 40 kV, 20 mA) [10, 11]. By examining the various diffraction rings with a Bausch and Lomb measuring magnifier with metric scale, one can count the differently shaped spots per ring segment (see Table III and Figs 14–17). Broadening of the Bragg diffraction of X-rays from a crystal with dislocations has been studied by Kyut [12].

2.3. Phase identification

For the determination of phase composition of the SiC whiskers, a retrofitted Philips Norelco vertical diffractometer was used. The goniometer has a graphite monochromator for the diffracted beam, an entrance slit 1.1 mm × 16 mm and an exit slit 0.5 mm × 16 mm, and a copper target X-ray tube operated at 40 kV, 20 mA. The output signal to the diffractometer recorder was interfaced directly with a Hewlett Packard HP-3350 series A/D converter coupled to an HP-3359 disk-based processor. The time constant was normally set at 2 s and the scale factor (full scale) at 2000 c.p.s. The recorded diffractograms were analysed by the procedure described elsewhere by the authors [13]. Fig. 18 shows selected portions of the respective diffractograms for SiC whiskers from Tokai, American Matrix, and Tateho. To obtain a better profile of the diffraction peak at the 0.266 nm spacing, a careful stepscan was run of the region 33°–35° (2θ); see Fig. 19. In addition to the diffractometer runs, film data were measured to substantiate the phase determination (see Table IV).

TABLE II Morphological data for SiC whiskers

Sample	Thickness (nm)	Length (nm)	Edges	Cavities	Inclusions	Stacking Faults (nm)	Twinning	Extra Features
Tokai	30–150	2000–20000	Smooth undulating	Nil		1.3–18 irregular	Intergrowth	Untapped packing density 0.059 g cm^{-3}
Tateho	50–500	1000–25000	Smooth (hexagonal cross-section)	Hollow Core (110 nm diameter)	(see Nutt [15])	~ 2		Large cluster of short whiskers, untapped packing density 0.114 g cm^{-3}
Am. Matrix	20–1000	1000–20000	Knobby (hexagonal cross-section			(n.a.)	Intergrowth	Clusters, untapped packing density 0.113 g cm^{-3}

TABLE III Crystallite-size distributions of SiC whiskers

Sample	(hkl)[a]	Number of spots	Shape of spots	Remarks
Tateho	$(1\,1\,1)_r$	20	Round (0.1 mm × 0.2 mm)	High background intensity between spots
		3	Rod-like (0.1 mm × 0.4 mm)	
	$(1\,1\,1)_l$	23	Round	
		2	Rod-like	
	$(2\,0\,0)_r$	5	Round (0.05 mm × 0.1 mm)	
		3	Rod-like (0.05 mm × 0.15 mm)	
	$(2\,0\,0)_l$	7	Rod-like (0.05–0.2 mm × 0.2–0.4 mm)	
		4	Round (0.1 mm × 0.2 mm)	
Tokai	$(2\,0\,0)_r$	47	Ellipsoidal (0.1 mm × 0.3 mm)	Moderate background intensity between diffraction spots
	(2 0 0)	43	Ellipsoidal (0.05 mm × 0.4 mm)	
	$(4\,2\,0)\alpha_1$	35	Round to ellipsoidal (0.05 mm × 0.4 mm)	
	$(4\,2\,0)\alpha_2$	24	As above	
American Matrix	$(1\,1\,1)_r$	5	Rod-like (0.05 mm × 0.6 mm)	Very low background intensity between diffraction spots
		32	Round (0.1 mm × 0.1 mm)	
		23	Ellipsoidal (0.2 mm × 0.4 mm)	
	$(4\,2\,0)\alpha_1$	10	Ellipsoidal (0.1 mm × 0.2 mm)	
		4	Rod-like (0.1 mm × 0.7 mm)	

[a] "r" refers to right side of centre; subscript "l", to left side.

To obtain phase data on individual SiC whiskers, it was necessary to employ SAED with the Jeol 1200 electron microscope. Fig. 20 is a three-fold enlargement of the pattern obtained from the Tokai SiC sample. The corresponding indexed data are given in Table V. Likewise, Fig. 21 and Table VI give SAED data for the Tateho samples and Fig. 22 and Table VII give SAED data for the American Matrix samples.

2.4. Oxidation rates

Weighed portions of SiC whiskers were loaded into small platinum cups and inserted into a DuPont thermogravimetric analyser (Model 951) with oxygen passing over the charge. The temperature was ramped at 10 °C min^{-1} to 1050 °C and held constant for 1200 min or longer. Figs 23 and 24 are the computer-plotted outputs of the thermogravimetric oxidations for American Matrix whiskers and for Tokai whiskers, respectively. In addition, oxidation of SiC whiskers was carried out in air at 1150 ± 25 °C for 5–25 h. The American Matrix whiskers gained 9.80 wt % after 5 h, 56.8 wt % after 25 h, and lost 4.58 wt % over the next 10 h. The Tokai whiskers gained 36.6 wt % after 5 h, 56.8 wt % after 20 h, and lost 0.20 wt % over the next 5 h. XRD analysis of the oxidized SiC revealed α-cristobalite and 5–10 wt % unreacted SiC. The Tateho whiskers, oxidized in air at 1105 °C (Netzsch unit) for 88 h, gained 48 wt %. No unreacted SiC was observed in the α-cristobalite formed. Surface area measurements by krypton adsorption (BET) revealed a reduction of surface area upon oxidation: Tateho, from 3.95 m^2 g^{-1} to 0.69 m^2 g^{-1}; Tokai, from 2.28 m^2 g^{-1} to 1.34 m^2 g^{-1}; and American Matrix, from 1.13 m^2 g^{-1} to 0.93 m^2 g^{-1}.

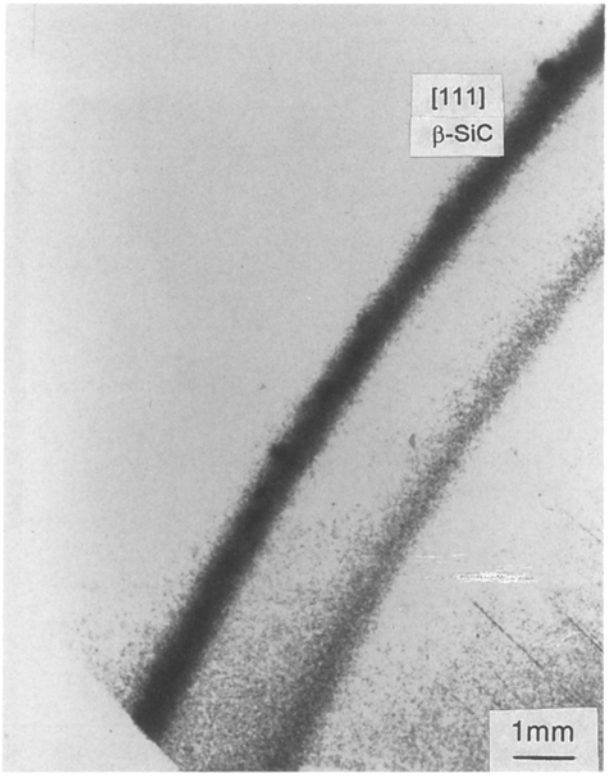

Figure 14 Ten-fold enlargement of the two innermost powder diffraction rings of Tateho SiC whiskers.

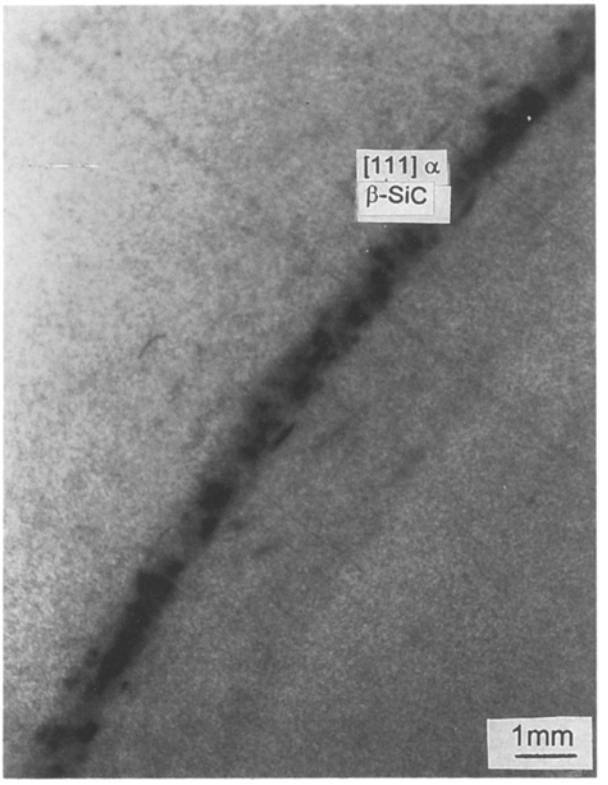

Figure 16 Ten-fold enlargement of the (1 1 1) β-SiC reflection from American Matrix SiC whiskers.

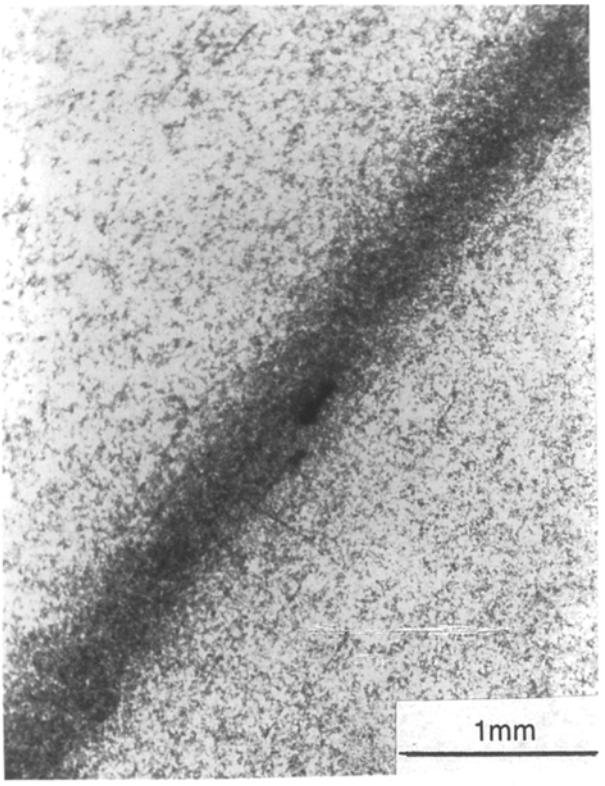

Figure 15 Thirty-fold enlargement of the 2 0 0 reflection of β-SiC from Tateho SiC whiskers.

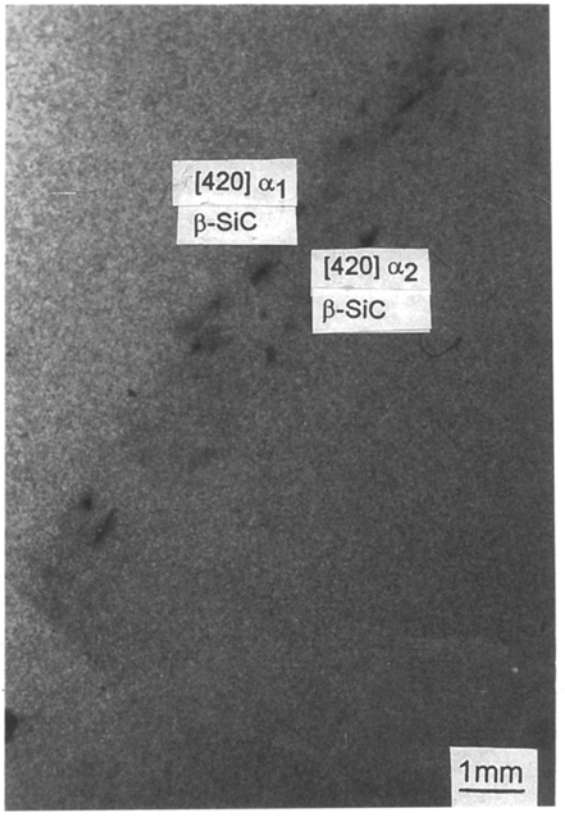

Figure 17 Ten-fold enlargement of the Cu$K_{\alpha_{1,2}}$ doublet of the (4 2 0) reflection from American Matrix SiC whiskers.

TABLE IV X-ray powder diffraction data for SiC whiskers (Tokai)

2θ (deg)	λ (nm)	d (nm)	β-SiC {hkl}	β-SiC I_p (arb. units)	β-SiC d_{calc} (nm)	β-SiC $(I_p)_{calc}$ (arb. units)	Minor phases
16.025	0.139222	0.2522	1 1 1	5, spotty	0.2517	(CuK_β)	
16.775	0.154184	0.2671		3, smooth			15R, 4H
17.213	0.154184	0.2605		2, spotty			6H
17.813	0.154184	0.2520	1 1 1	300, spotty	0.2517	300	
19.063	0.154184	0.2360		1, smooth			4H
20.650	0.154184	0.2186	2 0 0	50, spotty	0.2180	57	
22.575	0.154184	0.2008		10, spotty			Impurity phase(s)
26.325	0.154184	0.1738		1			Impurity phase(s)
26.813	0.154184	0.1709		3			Impurity phase(s)
29.950	0.154184	0.1544	2 2 0	120, spotty	0.1541	129	
31.913	0.154184	0.1458					
35.788	0.154184	0.13183	3 1 1	75, spotty	0.1315	81	
37.688	0.154184	0.12610		5	0.12584	12	
38.754	0.154184	0.12316		1			Impurity phase(s)
47.629	0.154184	0.10435		1			Impurity phase(s)
50.529	0.154184	0.09987	3 3 1	10, spotty	0.1000		
52.304	0.154184	0.09743	4 2 0	8, spotty	0.09748		
60.004	0.154056	0.08894	4 2 2	40, spotty	0.08899		
60.279	0.154439	0.08892	4 4 2	20, spotty	0.08899		
67.054	0.154056	0.08428	3 3 3	50, spotty	0.08390		
67.079	0.154439	0.08384	3 3 3	20, spotty	0.08390		

a_{obs} = 0.4364(7) nm, a_{lit} = 0.43597(1) nm.
Film data from Gandolfi camera with nickel-filtered CuK_α radiation.
θ = Bragg angle, λ = wavelength, d = interplanar spacing, I_p = peak intensity, a = cube edge of unit cell, $\{hkl\}$ = indices of reflection.

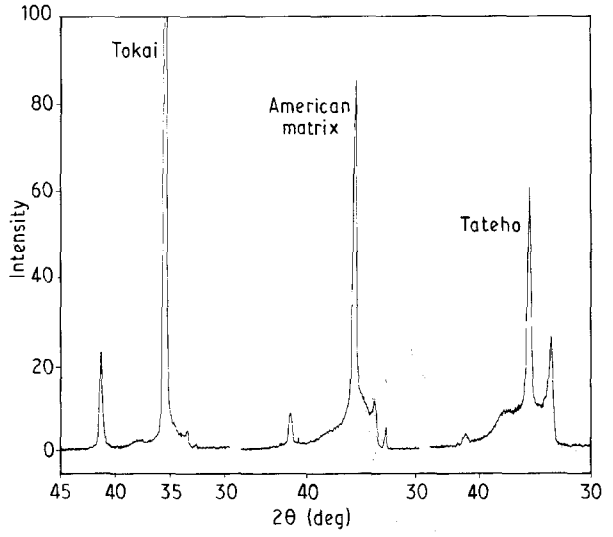

Figure 18 Diffractograms of the three different SiC whiskers.

TABLE V Electron diffraction data on Tokai SiC whiskers

r (mm)	d (nm)	{hkl}	d_{calc} (nm)
21.0	0.2517	1 1 1, $\bar{1}\bar{1}\bar{1}$, 1 1 $\bar{1}$, $\bar{1}\bar{1}$ 1	0.2517
24.3	0.2175	0 0 2, 0 0 $\bar{2}$	0.2180
34.0	0.1555	2 2 0, $\bar{2}\bar{2}$ 0	0.15412
42.0	0.1259	2 2 2, $\bar{2}\bar{2}\bar{2}$, 2 2 $\bar{2}$, $\bar{2}\bar{2}$ 2	0.12584
52.9	0.09942	$\bar{3}\bar{3}$ 1	0.10001
59.1	0.08944	$\bar{2}\bar{2}\bar{4}$	0.08898
63.0	0.08390	$\bar{3}\bar{3}\bar{3}$	0.08389
68.7	0.07694	$\bar{4}\bar{4}$ 0	0.07706
			a_{obs} = 0.4362(13) nm

r = radial distance of diffraction spot from central spot (primary beam); d = interplanar spacing; camera constant = $L\lambda$ = 5.286 mm nm; $\{hkl\}$ = indices for diffraction spots; $a_{\beta\text{-SiC}}$ = 0.43593(6) nm. Electron beam parallel to [0 1 1] zone axis.

3. Results and discussion

3.1. Chemical composition

As seen from Table I, the sum of the elements for the Tateho whiskers is 97.34 wt %; for the Tokai whiskers, 99.25 wt %, and for the American Matrix whiskers, 98.7 wt %. The quantitative data for the minor elements were taken from Karasek *et al.* [14]. The discrepancy of 2.66 wt % (Tateho) and 1.3 wt % (American Matrix) may be attributed to a low value for silicon, or a low value for oxygen, or both, or missed elements (e.g. nitrogen). Assuming that the carbon analyses are accurate within ± 0.2 wt % and that all the carbon is combined with silicon, one can calculate the SiC assay as 97.48% (Tateho), 96.81% (Tokai), and 98.15% (American Matrix). If one assumes the silicon analyses as correct and all of the silicon is combined as SiC, then the assay values for SiC are 95.94% (Tateho), 98.27% (Tokai), and 96.03% (American Matrix). However, the literature informs us that the oxygen is combined with silicon to form an Si–O–C "glass". Hence, correcting for some of the silicon combined as Si–C–O, one arrives at the following respective assay values: 94.74%, 95.83% and 93.02%. Upon complete oxidation in oxygen or air at temperatures above 1000 °C, the theoretical weight gain of pure SiC should be 49.85%. The observed gain of 56.8 wt % is difficult to explain in view of the fact that some SiC was not oxidized. The presence of impurities or the condensation of furnace volatiles on

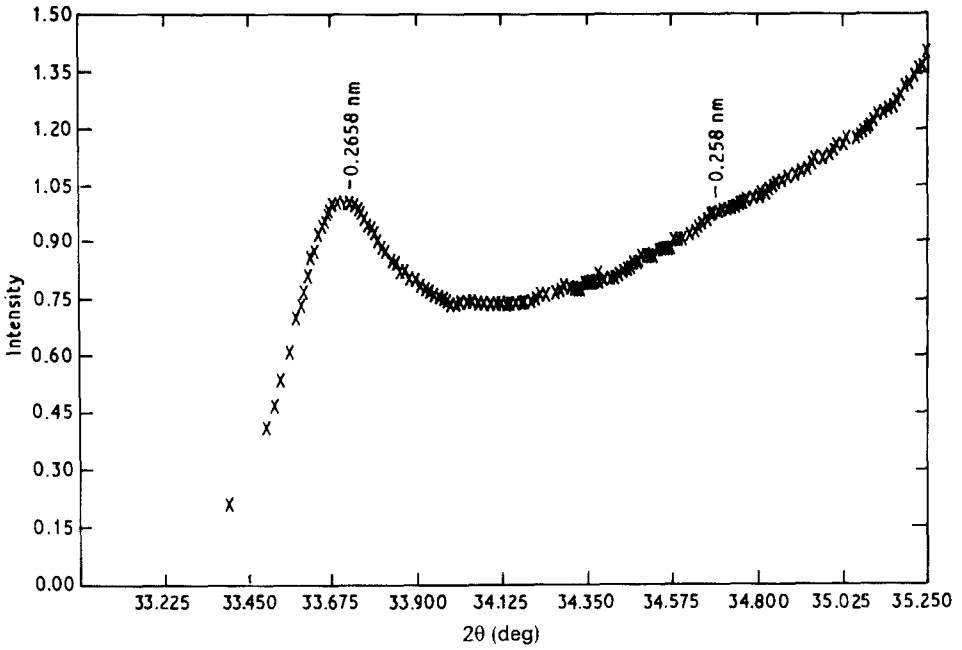

Figure 19 Stepscan of diffraction region between 33° and 35° (2θ) of American Matrix SiC whiskers.

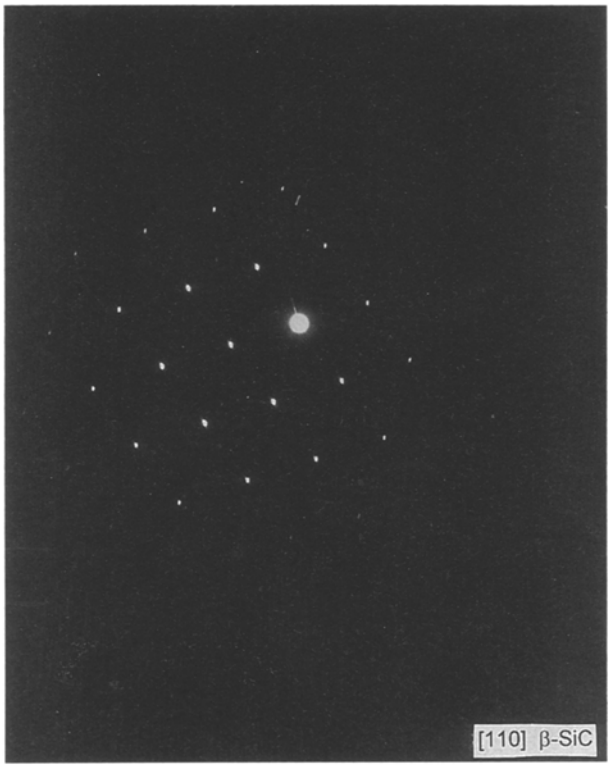

Figure 20 Electron diffraction pattern (SAED) from a single SiC whisker (Tokai).

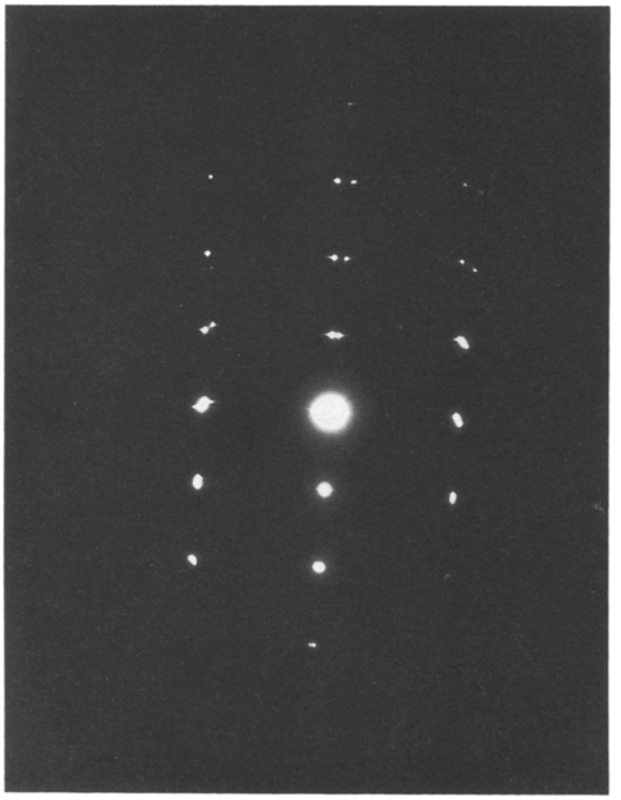

Figure 21 Electron diffraction pattern (SAED) from a single SiC whisker (Tateho).

the formed silica may allow a more-than-calculated weight gain. For the Netsch data (48 wt % gain), no such anomaly obtained.

3.2. Morphological aspects

The macroscopic shapes of the various SiC whiskers are clearly displayed in Figs 1–7. Light grinding did not affect the thickness of the whiskers but did shorten their length (Fig. 2). The Tateho sample contained the largest number of clusters of the type shown in Fig. 3. Variation in the thickness of the whiskers is readily recognized in Fig. 4 for Tokai whiskers. Surface roughness (or smoothness) is not uniform as seen in Fig. 5. The American Matrix whiskers exhibit rather knobby surfaces (see Figs 6 and 7). The hexagonal cross-section of the crystalline striated whiskers is easily identified in Fig. 7. The aspect ratio (length to

TABLE VI Electron diffraction data on Tateho SiC whiskers

r (mm)	d (nm)	$\{hkl\}$	d_{calc} (nm)
20.8	0.2513	111, $\bar{1}\bar{1}\bar{1}$	0.2517
34.2	0.1528	202, $\bar{2}0\bar{2}$	0.1541
39.78	0.1314	311, $\bar{3}\bar{1}\bar{1}$	0.13144
41.5	0.1260	222, $\bar{2}\bar{2}\bar{2}$	0.12584
53.7	0.09734	420, $\bar{4}\bar{2}0$	0.09734
62.3	0.08390	333, $\bar{3}\bar{3}\bar{3}$	0.08389
70.9	0.07372	531	0.07369
83.8	0.06298	444	0.06292
			a_{obs} = 0.4354(10) nm

r = radial distance of diffraction spot from central spot (primary beam); d = interplanar spacing; $\{hkl\}$ = indices for diffraction spot; Camera constant = $L\lambda$ = 5.227 mm nm; $a_{\beta SiC}$ = 0.43593(6) nm. Electron beam parallel to [1 1 2] zone axis.

Figure 22 Electron diffraction pattern (SAED) for a single SiC whisker (American Matrix).

thickness) ranges from 20–150. Metric data on the different whiskers are recorded in Columns 2 and 3 of Table II. The TEM data are particularly revealing for the Tateho whiskers (see Figs 8–10) which were found to possess hollow cores containing some debris. This finding is in agreement with Karasak's STEM photographs of a Tateho whisker cross-section (ultramicrotomed sample). Fig. 11 depicts faceting and intergrowth of whiskers. All of the whiskers examined exhibited irregular stacking faults normal to the whisker axis. For the Tokai whiskers (Fig. 12) the striations varied from 1.3–18 nm, indicating extended ordering for the larger uniform "bands". Fig. 13 clearly shows the thin (3 nm) coating on the American Matrix SiC whiskers.

3.3. Phase composition

The diffractograms of the three samples of SiC whiskers show strong patterns of crystalline β-SiC, however, with varying degrees of disorder (stacking faults) (Fig. 18). The Tokai whiskers consist of 95(3) wt % β-SiC of relatively low disorder, 3(1) wt % SiC(15R), and 2(1) wt % SiC(4H). The presence of a low concentration (approximately 1%) of the SiC (6H) polytype could not be ruled out. The American Matrix whiskers are composed of 85(5) wt % β-SiC with moderate disorder, 9(3) wt % SiC(6H), and 6(3) wt % SiC(15R). The Tateho SiC whiskers definitely show a much lower concentration of highly disordered β-SiC (approximately 60(10) wt %). The

TABLE VII Electron diffraction data on American Matrix SiC whisker

r (mm)	d (nm)	$\{hkl\}$	$d_{calc.}$ (nm) for cubic SiC(3C)
32.8	0.2520	111. $\bar{1}\bar{1}\bar{1}$, $11\bar{1}$, $\bar{1}\bar{1}1$, $1\bar{1}1$, $\bar{1}1\bar{1}$	0.2517
37.9	0.2181	002, $00\bar{2}$, 200, $\bar{2}00$	0.2180
53.8	0.1536	220, $\bar{2}\bar{2}0$, 202, $\bar{2}0\bar{2}$	0.1541
62.9	0.1314	311, $\bar{3}\bar{1}\bar{1}$, $31\bar{1}$, $\bar{3}1\bar{1}$, $\bar{3}11$, $3\bar{1}\bar{1}$, $3\bar{1}1$, $\bar{3}1\bar{1}$	0.13144
65.6	0.1260	222, $\bar{2}\bar{2}\bar{2}$. $22\bar{2}$, $\bar{2}\bar{2}2$, $2\bar{2}2$, $\bar{2}2\bar{2}$	0.12584
75.9	0.1089	004, $00\bar{4}$	0.10898
82.8	0.09983	331	0.10001
		H K L	d_{calc} (nm) for rhombohedral SiC(21R)
30.9	0.2675	$\bar{1}0\bar{1}$	0.2658
31.4	0.2632	$0\bar{1}\bar{2}$	0.2648
31.7	0.2608	$\bar{1}0\bar{4}$	0.2609
32.0	0.2583	$0\bar{1}\bar{5}$	0.2581
33.4	0.2475	018	0.2468
34.8	0.2375	1-0-10	0.2376
35.4	0.2335	0-1-11	0.2327
37.1	0.2228	1-0-13	0.2226

r = radial distance of diffraction spot from central spot (primary electron beam), d = interplanar spacing, hkl = indices for cubic SiC, HKL = indices for rhombohedral SiC(21R), Camera constant $L\lambda$ = 82.66 mm nm, $a_{\beta SiC}$ = 0.43593(6) nm. The lattice constants for the SiC(21R) polytype are a = 0.307 3 nm, c = 5.278 nm.

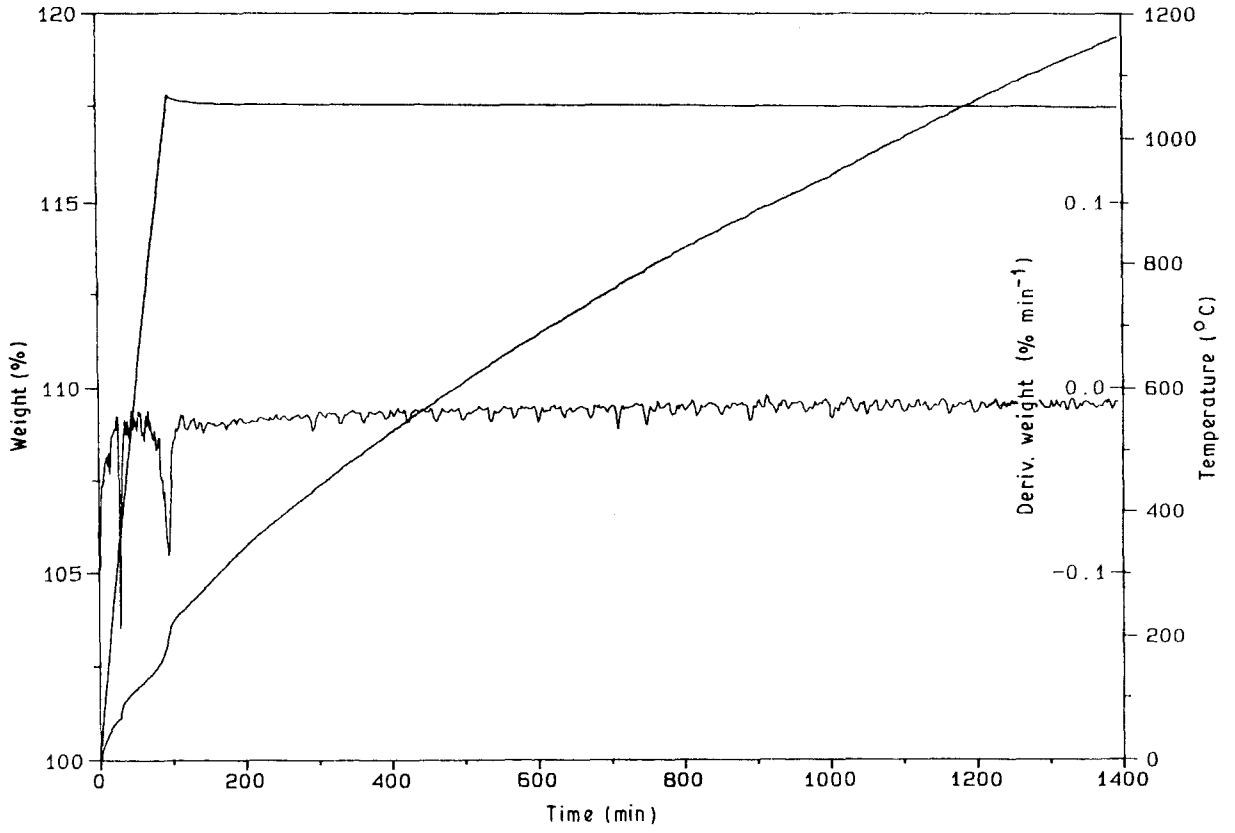

Figure 23 TGA plot of oxidation of American Matrix SiC whiskers.

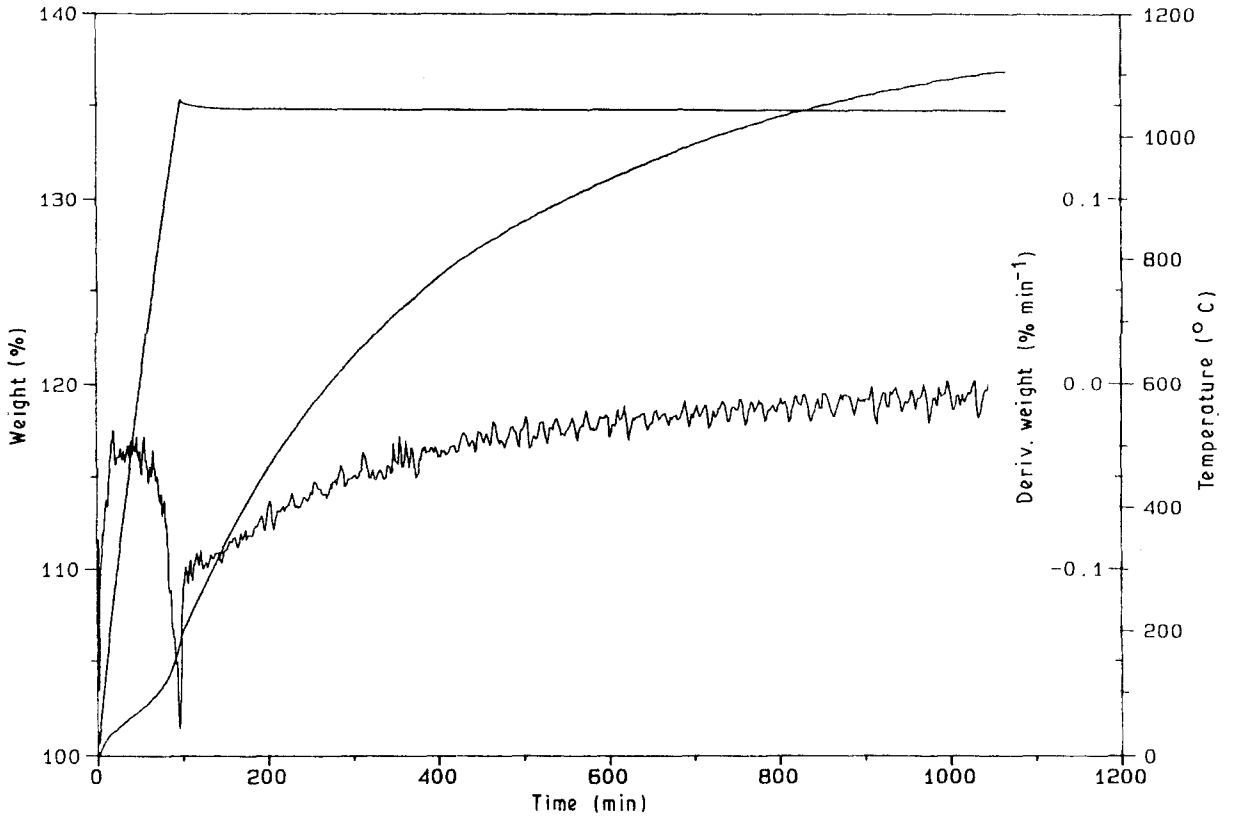

Figure 24 TGA plot of oxidation of Tokai SiC whiskers.

relative intensity of 2 0 0 reflection falls with increasing degree of disorder as documented in Table VIII. By contrast, the relative intensities of the 2 2 0 and 3 1 1 reflections increase with the degree of disorder. If the atomic coordinates of the disordered structure were known (or postulated), one could compute the corresponding diffraction pattern by using the Debye scattering function applied to a 5 nm cube of the

TABLE VIII Comparison of relative intensities of X-ray diffraction peaks for β-SiC whiskers

	PDF 29-1129		β-SiC		Tokai		Am. Matrix		Tateho	
$\{hkl\}$	d_{obs} (nm)	$(I/I_1)_{obs}$	d_{calc} (nm)	$(I/I)_{calc}$	d_{obs} (nm)	$(I/I)_{obs}$	d_{obs} (nm)	$(I/I_1)_{obs}$	d_{obs} (nm)	$(I/I_1)_{obs}$
1 1 1	0.252	1.00	0.2517	1.00	0.252	1.00	0.2516	1.00	0.2527	1.00
2 0 0	0.218	0.20	0.2180	0.19	0.218	0.16	0.2175	0.10	0.2187	0.06
2 2 0	0.1541	0.35	0.15412	0.43	0.1542	0.43	0.1540	0.62	0.1545	0.77
3 1 1	0.13140	0.25	0.13144	0.27	0.1315	0.29	0.1313	0.40	0.1318	0.39

$\{hkl\}$ = indices of reflection for the cubic polytype of SiC. The standard pattern for β-SiC is given in Columns 2 and 3; the calculated pattern is based on the 2, 2*F*43*m*(4) structure and a lattice constant of $a = 0.43593(6)$ nm.

disordered structure. In addition to the low concentrations of non-cubic SiC polytypes, a few very weak reflections pertaining to some unidentified impurities may be detected. From the total minor elements quantitated, one can conclude that the non-SiC impurities (such as silicates like gehlenite, $Ca_2Al_2SiO_7$) are less than 2 wt %.

3.4. Crystallite-size distribution

Because diffractometer traces do not reveal "graininess" of a diffraction line, one resorts to film methods to obtain two-dimensional details of the various diffraction rings. Thus, the powder diffraction film for Tokai whiskers (as-received) yields pertinent information on the presence of "coarse" crystallites in the presence of small (approximately 30 nm) crystallites. It also reveals that the crystallites for the (15R) and (4H) polytypes yield smooth diffraction rings. The data of Table IV show that the Tokai SiC whiskers consist predominantly of β-SiC, minor concentrations of SiC(15R) and SiC(4H), and some minor unidentified impurity phase(s). As no internal calibrant was employed, one should not expect better agreement between the observed and calculated *d*-values. The measurements for the diffraction spots within the recorded segment of several diffraction rings are detailed in Table III (see also Figs 14–17). For the Tateho whiskers, the high homogeneous intensity of a diffraction ring is attributed to a large number of small crystallites of β-SiC (approximately 20–30 nm). Only roughly 5% of the diffracted intensity pertains to the measured diffraction spots. It is also evident that one is dealing with an essentially bimodal distribution of round and rod-like "coarse" crystallites. The approximate 100-fold enlargement of the projected image of a coarse crystallite is caused by the divergence of the primary X-ray beam and by the halation of the intense diffraction spot. However, the aspect ratio of any rod-like spot (ranging from 3–12) is certainly much smaller than the macroscopic aspect ratio (20–150) of any single whisker. This difference signifies that any single whisker is not a single crystal. With finer grain film and more parallel radiation, it should be possible to obtain diffraction spots from crystallites of less than 100 nm diameter.

3.5. Electron diffraction results

The advantage of SAED is the capability of obtaining diffraction data from a single SiC whisker. From the excellent single-crystal patterns shown in Figs 20 and 21 it was a straightforward procedure to index and identify the β-SiC phase (see Tables VI and VII). Although no SAED patterns were obtained with the electron beam parallel to the [0 1 1] zone axis, such a pattern was registered by Nutt [15]. His pattern shows continuous streaking along the β-SiC reciprocal lattice rows, this smearing of the diffracted X-rays is caused by finely spaced planar defects oriented normal to the whisker-growth direction. Such diffuse scattering was first interpreted by Jagodzinski and Arnold [16], who studied single crystals of β-SiC formed by vapour deposition. SAED patterns (see Table VIII) confirmed that the American Matrix whiskers are composed predominantly of cubic β-SiC. In addition, planar faults were observed to extend normal to the whisker axis and align along (1 1 1) planes. Electron diffraction patterns recorded from this whisker provided evidence for two types of planar defects: (i) a twin boundary parallel to (1 1 1), and (ii) the presence of a SiC(21R) polymorph. Direct evidence for these two defects is present in a diffraction pattern (shown in Fig. 22) where the twin axis is identified as [1 1 1]. Furthermore, the streaks normal to the common (1 1 1) plane are composed of an array of faint reflections whose periodicity corresponds to the (21R) polytype.

3.6. Oxidation rates

At a constant temperature, the rate of oxidation of the SiC whiskers should vary directly with the exposed surface areas, *S* (expressed in m^2), and the specific rate of oxidation per square metre per second, σ_s, and exponentially with the energy of activation, ΔE, for the reaction $SiC(surface) + 2O_2 \rightarrow SiO_2(surface) + CO_2$. Hence, the rate of oxidation, r_{ox}, can be expressed by

$$r_{ox} = \sigma_s S \exp(^{\Delta E}/_{RT}) \quad (1)$$

In the thermogravimetric oxidation, the surface, *S*, is continuously decreasing while the SiO_2 coating is increasing with time. If the silica coating is non-porous, then the rate-controlling step is the rate of oxygen diffusion through this layer. The gradual oxidation of the American Matrix SiC whiskers transforms them into crystalline α-cristobalite whiskers of the original shape (but slightly dilated) (Fig. 25). In the case of the Tokai whiskers, the oxidized SiC is transformed into amorphous SiO_2 of the same shape

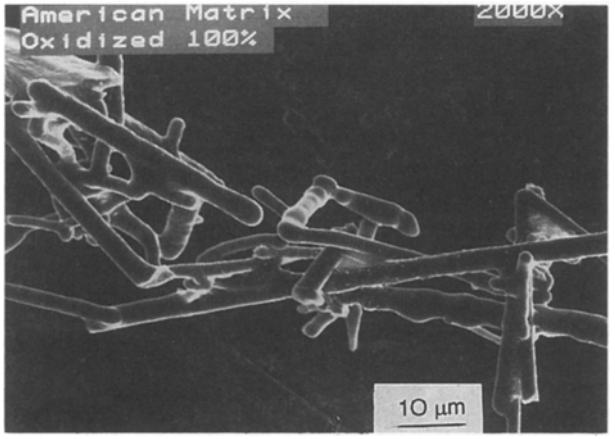

Figure 25 Scanning electron micrograph of oxidized SiC whiskers (American Matrix).

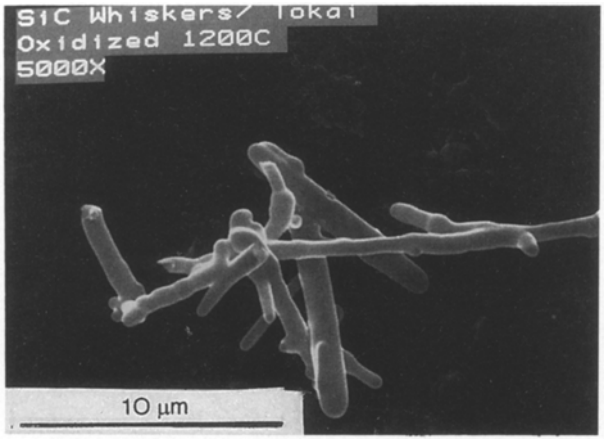

Figure 26 Scanning electron micrograph of oxidized SiC whiskers (Tokai).

(Fig. 26). Although the weight gain after 20 h in air at 1150 °C is greater than the theoretical gain of 49.85 wt %, some residual unoxidized SiC remained (5%–10%). The much slower rate of oxidation of the American Matrix whiskers may be due to either the thin (3 nm) amorphous coating on the whiskers or the lower surface area of the thicker whiskers or both factors. The chemical kinetics of the oxidation will be addressed in a separate communication.

4. Conclusions

For the three commercial SiC whiskers examined, the single SiC whiskers are not single crystals. They consist predominantly of disordered cubic SiC with minor concentrations of (6H), (4H), and (15R) polytypes all incorporated along the whisker axis (growth axis). The crystallite-size distribution of Tateho whiskers is essentially a bimodal distribution with approximately 5% being coarse crystallites (> 200 nm) and the balance 30 nm or less in average diameter. The American Matrix whiskers are characterized by a multimodal distribution of coarse crystallites with some crystallite sizes in the 30 nm range. The Tokai whiskers can be described as intermediate to the other two types of whisker. In all three cases, the concept of bounded discrete crystallites within a physical mixture of polytypes is inappropriate. Rather, one should perceive the extent of the contiguous regions of ordered (disordered) polytypes as the equivalent of a crystallite size.

Although the external morphology of the three SiC whiskers is quite similar, one notes the following differences: (i) the Tateho whiskers (grown during the pyrolysis of silica and carbon produced from ground rice hulls) are hollow and possess many dense clusters; (ii) the American Matrix whiskers are somewhat coarser than the other two SiC whiskers and possess a very thin (3 nm) amorphous coating. This coating very likely will affect its interfacial properties with matrix powders used for producing composites. Likewise, the slower rate of oxidation of the American Matrix whiskers may be attributed to this coating.

Acknowledgement

The authors are grateful to Dr David Susnitzky for the excellent TEM and SAED data.

References

1. G. C. WEI and P. F. BECHER, *Amer. Ceram. Soc. Bull.* **64** (1985) 298.
2. *Idem, J. Amer. Ceram. Soc.* **67** (1984) C267.
3. J. HOMENY, W. L. VAUGHN and M. K. FERBER, *Amer. Ceram. Soc. Bull.* **66** (1987) 333.
4. S. T. BULJAN, J. G. BALDON and M. L. HUCKABEE, *ibid.* **66** (1987) 347.
5. A. H. CHOKSHI and J. R. PORTER, *J. Amer. Ceram. Soc.* **68** (1985) C144.
6. K. R. KARASEK *et al., J. Mater. Sci.* **24** (1989) 1617.
7. K. R. KARASEK *et al., J. Amer. Ceram. Soc.* **72** (1989) 1907.
8. T. N. TIEGS, P. F. BECHER and L. A. HARRIS, in "Ceramic microstructures 1989: role of interfaces", Material Science Research Series, No. 21, edited by J. A. Pask and A. G. Evans (Plenum Press, New York, NY, 1987) pp. 911–18.
9. S. BRADLEY *et al., J. Amer. Ceram. Soc.* **72** (1989) 628.
10. L. K. FREVEL, D. C. De LEEUW and W. R. ALBE, *Norelco Reporter* **29**(2) (1982) 28.
11. L. K. FREVEL, *Adv. X-ray Anal.* **27** (1984) 3.
12. R. N. KYUT, *Sov. Phys. Crystallogr.* **33** (1988) 488.
13. L. K. FREVEL, D. R. PETERSEN and C. K. SAHA, *J. Mater. Sci.* (1991) in press.
14. K. R. KARASEK *et al.*, Allied-Signal Engineered Materials Research Center, Des Plaines, IL (1988).
15. S. R. NUTT, *J. Amer. Ceram. Soc.* **71**(3) (1988) 149.
16. M. JAGODZINSKI and H. ARNOLD, in "Proceedings of the Conference on Silicon Carbide", Boston, MA, 2–3 April 1959, edited by J. R. O'Conner and J. Smittens (Pergamon Press, New York, 1960) pp. 130–45.

Received 15 October 1991
and accepted 20 August 1992